APL Materials

Experimental study on coupled caloric effect driven by dual fields in metamagnetic Heusler alloy $Ni_{50}Mn_{35}In_{15}$

Cite as: APL Mater. **7**, 051102 (2019); https://doi.org/10.1063/1.5090599
Submitted: 29 January 2019 . Accepted: 12 April 2019 . Published Online: 06 May 2019

Fei-Xiang Liang, Jia-Zheng Hao, Fei-Ran Shen, Hou-Bo Zhou, Jing Wang, Feng-Xia Hu, Jun He, Ji-Rong Sun, and Bao-Gen Shen

Experimental study on coupled caloric effect driven by dual fields in metamagnetic Heusler alloy $Ni_{50}Mn_{35}In_{15}$

Cite as: APL Mater. 7, 051102 (2019); doi: 10.1063/1.5090599
Submitted: 29 January 2019 • Accepted: 12 April 2019 •
Published Online: 6 May 2019

Fei-Xiang Liang,[1,2] Jia-Zheng Hao,[1,3] Fei-Ran Shen,[1,2] Hou-Bo Zhou,[1,2] Jing Wang,[1,2,a)] Feng-Xia Hu,[1,2,4,a)] Jun He,[3] Ji-Rong Sun,[1,2,4] and Bao-Gen Shen[1,2,4]

AFFILIATIONS

[1]Beijing National Laboratory for Condensed Matter Physics and State Key Laboratory of Magnetism, Institute of Physics, Chinese Academy of Sciences, Beijing 100190, People's Republic of China
[2]School of Physical Sciences, University of Chinese Academy of Sciences, Beijing 100049, People's Republic of China
[3]Division of Functional Material Research, Central Iron and Steel Research Institute, Beijing 100081, People's Republic of China
[4]Songshan Lake Materials Laboratory, Dongguan, Guangdong 523808, People's Republic of China

[a)]**Authors to whom correspondence should be addressed:** fxhu@iphy.ac.cn and wangjing@iphy.ac.cn

ABSTRACT

The multicaloric and coupled caloric effect of metamagnetic shape memory alloy $Ni_{50}Mn_{35}In_{15}$ driven by hydrostatic pressure and magnetic field has been systematically investigated. The existence of pressure significantly changes the relationship between the magnetic volume coupling coefficient and temperature. Thermodynamic analysis indicates that the magnetocaloric effect at a certain pressure is equivalent to the magnetocaloric effect at ambient pressure adjusted by the coupled caloric effect (ΔS_{cp}). This theoretical result is verified by magnetic measurements under various pressures for the $Ni_{50}Mn_{35}In_{15}$ with the inverse magnetocaloric effect. When a pressure of 0.995 GPa is applied, the peak value of entropy change can be as high as $|\Delta S| \sim 25.7\ J\ kg^{-1}\ K^{-1}$ upon a magnetic field change of 5–0 T, which increases by 8% compared to that of ambient pressure though the magnetization change (ΔM) across martensitic transition reduces 20% owing to the shift of the transition to higher temperature by 30 K. Detailed analysis indicates that the coupled caloric effect involving the strengthened magnetostructural coupling under pressure is responsible for the enhanced entropy change. The quantitative analysis of cross coupling term driven by dual fields reveals the essence of regulated magnetocaloric effect by pressure, which will be helpful for designing new materials based on the magnetostructural coupling strength.

Caloric materials have received a widespread attention in the last decades due to their potential application in solids' refrigeration. For spin-lattice coupled materials, changing the external field can change the order of alignment and exhibit a giant caloric effect. Since Pecharsky and Gschneidner reported the giant magnetocaloric effect in $Gd_5Si_2Ge_2$ with first-order phase transition (FOPT) involving magnetostructural coupling,[1] FOPT materials with magnetostructural transition have been extensively studied, and a series of magnetocaloric materials such as $LaFe_{13-x}Si_x$-based alloys,[2] MnAs,[3] and Ni–Mn–Ga[4] have been discovered. In particular, since the ferroic order parameter is generally coupled with the crystal lattice, the magnetocaloric materials with FOTP are also expected to show mechanocaloric (barocaloric and elastocaloric) effects, such as La(Fe, Co, Si)$_{13}$,[5] Ni–Mn–In,[6] and Ni–Co–Mn–Sn.[7] As a clean and effective means, hydrostatic pressure can directly change the electronic structure and the magnetic structure by modifying lattice parameters, which is of great significance for observing new physical phenomena.[8]

Multicaloric materials, referring to the thermal changes driven by more than one type of external fields, have been extensively studied in recent years.[6,7,9] Accordingly, the coupled caloric effect was theoretically studied from different angles, such as Landau phase

transition theory[10,11] and thermodynamic analysis.[9] Compared to the monocaloric effect, the multicaloric effect has specific advantages: (1) FOTP driven by more than one field can give a larger parameter space, for example, a lower field may become accessible to drive the phase change, (2) widening the phase transition temperature window to achieve caloric effects over a wider temperature range,[9,12] and (3) eliminating the hysteresis by transferring from one control field to another.[13]

The stoichiometric $Ni_{50}Mn_{25}In_{25}$ crystallizes in a body-centered cubic $L2_1$ structure. Ni atoms occupy the apex position, while Mn atoms and In atoms occupy the body center position in turn.[14] The magnetic moments mainly localize at Mn atoms which have been proved to be ferromagnetically coupled by indirect exchange interaction.[14–16] The phase diagram of $Ni_{50}Mn_{25+x}In_{25-x}$ ($0 \le x \le 20$) has been studied by Sutou *et al.*,[17] which shows only a second order phase transition from high temperature paramagnetic (PM) phase to low temperature ferromagnetic (FM) phase during cooling in stoichiometric $Ni_{50}Mn_{25}In_{25}$.[17] However, for the Mn-riched $Ni_{50}Mn_{25+x}In_{25-x}$ alloys, the excess of Mn atoms will occupy the position of the In atoms, resulting in the shortening of partial Mn–Mn neighbor distance from the original $\frac{\sqrt{2}a}{2}$ (a is the lattice parameter) to $\frac{a}{2}$. As a result, the corresponding Mn–Mn interaction is changed from the original ferromagnetic type to the antiferromagnetic type.[15] And a first-order martensitic transition induced by the temperature or magnetic field from a cubic $L2_1$ high-temperature phase (austenite) to a lower symmetry low-temperature phase (martensite) with several possible structures depending on composition and elements[17] can be realized.[18] In a review article,[19] Dubenko *et al.* carefully summarized the magnetic, magnetocaloric, magnetotransport, and magneto-optical properties of Ni–Mn–In-based Heusler alloys with various forms including bulk, ribbons, and microwires. These properties can be optimized through variations in stoichiometry, chemical substitution, and fabrication parameters or postprocessing. The Ni–Mn–In alloys exhibiting multifunctional properties deserve further investigations. The enhancement of magnetocaloric effect by partial substitution of In by Si in $Ni_{50}Mn_{35}In_{15}$ has been reported by Pathak *et al.*[20] Our previous work showed that for $Ni_{50}Mn_{35.2}In_{14.8}$, during the cooling process, the FOPT is from the cubic $L2_1$ structure to the modulated 7M tetragonal martensite phase.[21] Moreover, as the Mn content increases, the martensitic transformation temperature increases rapidly. This is because in the temperature region where the parent and martensite phases coexist, the contribution of the magnetic phase in the Gibbs free energy are varied when the two phases reach equilibrium.[17]

On the other hand, the hydrostatic pressure will also reduce the lattice parameters and the Mn–Mn distance, resulting in the enhancement of the antiferromagnetic exchange interaction between Mn atoms in $Ni_{50}Mn_{35}In_{15}$.[8] Therefore, the presence of hydrostatic pressure can also lead to an increase in the martensitic transformation temperature in $Ni_{50}Mn_{35}In_{15}$. Considering that the ferroic order parameter is strongly coupled with lattice, the volume will also change greatly along with the change of magnetic properties during the martensitic transformation. Therefore, the thermal effect in the pressure-driven phase transition process is attracting more and more attention.[6] However, there are few experimental research for the coupled caloric effect driven by dual fields, particularly for the Ni–Mn–In Heusler alloys showing the inverse magnetocaloric effect.

Here, we report multicaloric and coupled caloric effect driven by the magnetic field and hydrostatic pressure in the off-stoichiometric $Ni_{50}Mn_{35}In_{15}$ alloy, which shows a FOPT from high-temperature austensite to low-temperature martensite. Application of hydrostatic pressure enhances antiferromagnetic coupling between Mn atoms, which in turn leads to an increase of the martensitic transformation temperature.[17] In the temperature region of phase transition, the effect of pressure can be expressed by the pressure-driven magnetostructural transition, which causes the change of magnetism, that is, the pressure-induced change of magnetic volume coupling coefficient, $\chi_{12} = \left[\frac{\partial M}{\partial P}\right]_{T,\mu_0 H}$. The definition of χ_{12} is analogous to the magnetoelectric coupling coefficient driven by magnetic and electric fields for a magnetoelectric coupling system.[22] The coupled caloric effect is closely related to the magnetic volume coupling coefficient. The existence of pressure significantly adjusts the relationship between the magnetic volume coupling coefficient χ_{12} and temperature and thus affects the expression of the coupled caloric effect under different pressures. From the perspective of magnetic volume coupling, the evolution of χ_{12} with pressure reveals the intrinsic nature of the coupled effect. A challenge for solid-state refrigeration is to adjust operating temperature while maintain the amplitude of the caloric effect. In this paper, the study of the coupled caloric effect in $Ni_{50}Mn_{35}In_{15}$ explains the intrinsic nature of the pressure-regulated magnetocaloric effect and its temperature. It will be helpful for designing new materials based on χ_{12}, which closely correlates with the magnetostructural coupling strength.

Ni–Mn–In alloy with nominal composition $Ni_{50}Mn_{35}In_{15}$ is prepared by the arc melting method. The preparation process is the same as that described in Ref. 21. The commercial purities of Ni, Mn, and In are 99.9 wt. %, 99.9 wt. %, and 99.99 wt. %, respectively. Homogenization was achieved by remelting the ingots three times, then sealing the ingots into quartz ampoules under argon atmosphere, and annealing at 1073 K for 24 h, followed by quenching in ice water. Magnetic properties were measured by superconducting quantum interferometer device (SQUID, MPMS-7 T). Hydrostatic pressure was applied by using a Be–Cu pressure cell, where Daphne 7373 was used as the pressure transferring medium. The pressure inside the cell was calibrated by the shifts of the superconductive transition temperature of Pb, which is put together with the specimen during measurements. Since the specimen exhibits different hysteresis effects against temperature, magnetic field, and pressure during the first-order phase transition, the test process was performed by increasing pressure, decreasing temperature, and decreasing magnetic field, so as to eliminate the influence of possible inaccuracy on the measured results. Moreover, in the temperature region of phase transition, where two phases coexist for the materials with FOPT, an extrinsic spike of entropy change tends to arise if the isothermal magnetization curves (M-$\mu_0 H$) is measured without taking the history of the material into account.[23,24] By proper measurements eliminating the history, the M-$\mu_0 H$ curves can be used in calculating the entropy change. For Ni–Mn–In Heusler alloys, choosing the demagnetizing branch on cooling from above the transition can reliably calculate the entropy change.[24] Besides, using the thermomagnetic curves (M-T) measured under different magnetic fields can also eliminate the fake peak.[24,25] Based on this, we measured the M-T curves at the 220–340 K temperature range in cooling and demagnetizing processes to make ensure the reliable

calculation of entropy change. The sweep rate of temperature during the measurements was set as 1 K/min, and the entropy change in the phase transition process is calculated using the Maxwell relation.

The coupled caloric effect can be considered from a thermodynamic point of view.[9] Since entropy is a state function, its size is independent of the sequence and path of the driving fields.[12] For a phase transition process driven by a magnetic field change from 0 to $\mu_0 H$ and a pressure change from 0 to P, the entropy change can be expressed by the following path:

$$\Delta S[(0,0) \rightarrow (P,\mu_0 H)] = \Delta S[(0,0) \rightarrow (P,0)] + \Delta S[(P,0) \rightarrow (P,\mu_0 H)]. \quad (1)$$

The first term on the right denotes the entropy change upon changing the pressure from 0 to P in the case where the external magnetic field keeps 0, which is the monocaloric effect due to the application of pressure. The second term indicates the entropy change caused by the change of magnetic field from 0 to $\mu_0 H$ under the condition that the external pressure keeps P. We can express these two terms as follows:

$$\Delta S[(0,0) \rightarrow (P,\mu_0 H)] = \int_0^P \left[\frac{\partial M}{\partial T}\right]_{P',\mu_0 H=0} dP' + \int_0^{\mu_0 H} \left[\frac{\partial M}{\partial T}\right]_{P,\mu_0 H'} d(\mu_0 H'). \quad (2)$$

When expanding the second term on the right of Eq. (2),[9,11] we can get a new form of the expression as follows:

$$\int_0^{\mu_0 H} \left[\frac{\partial M}{\partial T}\right]_{P,\mu_0 H'} d(\mu_0 H') = \int_0^{\mu_0 H} \left[\frac{\partial M}{\partial T}\right]_{P=0,\mu_0 H'} d(\mu_0 H') + \int_0^P \int_0^{\mu_0 H} \frac{\partial \chi_{12}}{\partial T} dP' d(\mu_0 H'). \quad (3)$$

From Eqs. (1)–(3), the entropy change $\Delta S[(0, 0) \rightarrow (P, \mu_0 H)]$ can be expressed as follows:

$$\Delta S[(0,0) \rightarrow (P,\mu_0 H)] = \int_0^P \left[\frac{\partial M}{\partial T}\right]_{P',\mu_0 H'=0} dP' + \int_0^{\mu_0 H} \left[\frac{\partial M}{\partial T}\right]_{P=0,\mu_0 H'} d(\mu_0 H') + \int_0^P \int_0^{\mu_0 H} \frac{\partial \chi_{12}}{\partial T} dP' d(\mu_0 H'). \quad (4)$$

The first term on the right of Eq. (4) represents the entropy change of the monocaloric effect driven by pressure (in the absence of magnetic field); the second term represents the entropy change of the monocaloric effect driven by the magnetic field (in the absence of pressure); and the last term is the thermal effect of the magnetolattice cross coupling term, i.e., the coupled caloric effect, ΔS_{cp},

$$\Delta S_{cp} = \int_0^P \int_0^{\mu_0 H} \frac{\partial \chi_{12}}{\partial T} dP' d(\mu_0 H'). \quad (5)$$

Here, $\chi_{12} = \left[\frac{\partial M}{\partial P}\right]_{T,\mu_0 H}$ is the cross-susceptibility, which represents the magnetic volume coupling coefficient when the driving fields are pressure and magnetic field. The macroscopic physical meaning of χ_{12} refers to the change of magnetism caused by the phase transition, which is driven by the external pressure at a certain temperature in phase transition temperature region. While from the microstructural angle, it presents the enhancement of the antiferromagnetic exchange interaction due to the shortening of the Mn–Mn atomic distance by external pressure, and the enhanced magnetic contribution to Gibbs energy, which causes the phase transition temperature to move toward the higher temperature region.[17] By measuring the thermomagnetic curves at different magnetic fields and different pressures, the relationship between the magnetization and the pressure (M-P curve) at a specific temperature can be obtained. Then, the magnetic volume coupling coefficient χ_{12} can be deduced from the M-P curve by nonlinear fitting, and the coupled effect (ΔS_{cp}) can be calculated by Eq. (5). Meanwhile, from Eq. (3), we can know that for a FOPT driven by a magnetic field under a specific pressure, the entropy change is equivalent to the entropy change at ambient pressure adjusted by the coupled caloric effect.

Figure 1(a) shows the thermomagnetic curves measured at a magnetic field of 5 T during cooling process under different

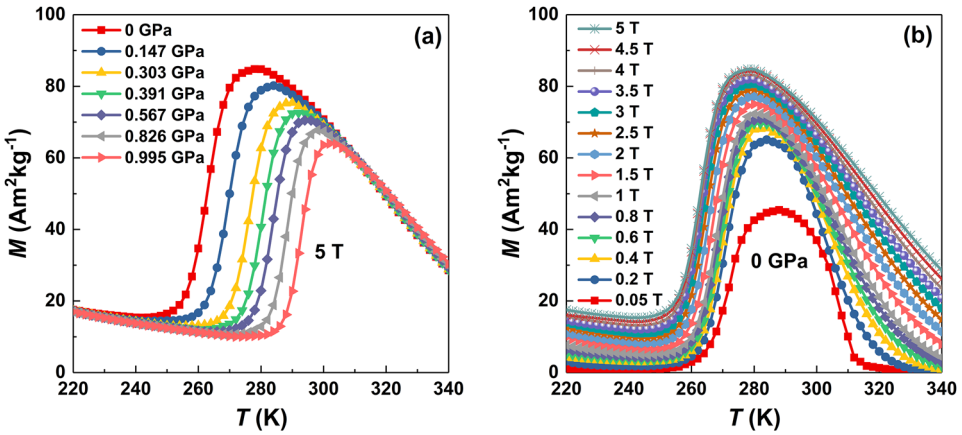

FIG. 1. Thermomagnetic curves measured on cooling (a) at a constant magnetic field of 5 T but different hydrostatic pressures, and (b) at a constant ambient pressure (0 GPa) but different magnetic fields.

hydrostatic pressures including 0, 0.147, 0.303, 0.391, 0.567, 0.826, 0.995 GPa (for clarity, ambient pressure here is defined as 0 GPa). It can be seen that during the cooling process, the specimen undergoes martensitic transformation, and the magnetization abruptly reduces from the ferromagnetic phase to the nonmagnetic phase.[26,27] In the vicinity of martensitic transition, the change of magnetization (ΔM) decreases with increasing pressure owing to the shift of the transition to higher temperature. Although the decreased ratio of ΔM is as large as ~20% with pressure increasing from 0 to 0.995 GPa, the total entropy change does not reduce but shows an increase by 8% owing to the contribution of the coupled caloric effect (see detailed discussion thereafter). Moreover, the increase of pressure makes the magnetostructural transition temperature (T_M) shift to a higher temperature, while the Curie temperature of the austenite phase ($T_C{}^A$) remains basically unchanged. Figure 1(b) shows the thermomagnetic curves during the cooling process under different magnetic fields at ambient pressure. As magnetic field increases, T_M shifts to lower temperature. As shown in Figs. 1(a) and 1(b), the martensitic transformation shifts to higher temperatures as the pressure increases, while it shifts to lower temperature as the magnetic field increases. This behavior can be explained by the fact that the magnetic field stabilizes the high temperature ferromagnetic phase and the pressure stabilizes the low temperature small volume phase.

Based on the M-T curves measured at 220–340 K temperature range under different magnetic fields and pressures, entropy change ΔS can be rationally calculated using Maxwell's relation as follows:[25,28]

$$\Delta S(T,\mu_0 H) = S(T,\mu_0 H) - S(T,0) = \int_0^{\mu_0 H} \left(\frac{\partial M(\boldsymbol{T},\mu_0 H')}{\partial T}\right)_{\mu_0 H'} d(\mu_0 H'). \quad (6)$$

Here, numerical integration is performed using a set of M vs T plots obtained with different applied $\mu_0 H$ [as shown in Fig. 1(b) for P = 0 GPa]. Using Eq. (6), the entropy change ΔS as a function of temperature (at constant pressures) for a field change of 5–0 T is calculated and shown in Fig. 2(a). It can be seen that as the pressure increases from 0 to 0.995 GPa, the ΔS peak shifts to high temperature by 30 K from 264 K to 294 K, which is consistent with Fig. 1(a), indicating the notable tunability of phase transition temperature by pressure. More importantly, the peak value of $|\Delta S|$ increases from 23.8 J kg^{-1} K^{-1} to 25.7 J kg^{-1} K^{-1} by 8% though the change of magnetization (ΔM) across phase transition reduces 20% as a pressure of 0.995 GPa is applied [Fig. 1(a)]. This is attributed to the contribution of strengthened magnetic-structural coupling by pressure, which is expressed by the coupled caloric effect. Figure 2(b) shows the first-order differential of the thermomagnetic curves at 0 GPa and 0.995 GPa measured at 5 T. The peak of dM/dT under 0.995 GPa is narrower and higher than that of 0 GPa, which means that the former presents a sharper transition. This also indicates that the increase of pressure strengthens the magnetic-structural coupling, and hence enhances the first-order nature of phase transition properties to some extent, consistent with the results of the finite element simulation reported previously.[29]

The positive entropy change around 310 K is derived from the paramagnetic-ferromagnetic phase transformation of austenite. The increase in pressure does not show much influence on the Curie temperature, $T_C{}^A$. But at high pressures, the martensitic temperature T_M goes close to $T_C{}^A$ [see Fig. 1(a)]. That is to say, the ferromagnetic ordering of austenite has not been well aligned when the martensitic transformation occurs; hence, the change of magnetization across the $T_C{}^A$ reduces under high pressure. This should be the cause of the slight reduction of $|\Delta S|$ around ~310 K with increasing pressure.

We collected a series of experimental data by performing magnetic measurements under several constant pressures, 0, 0.147, 0.303, 0.391, 0.567, 0.826, 0.995 GPa. The numerical analysis of the coupled caloric effect involves differential and integration, that is, continuous data are desired throughout the phase transition. Numerical simulation is performed to obtain the continuous M-P curves in the phase transition region, where nonlinear fitting was employed. For the M-P curves in the phase transition region, magnetization M exhibits the characteristics of the tanh function with pressure P. We found that the fitted M-P curves by tanh function are highly consistent with the actually measured data. Under a constant magnetic field (for example, 5 T) and a specific temperature, we

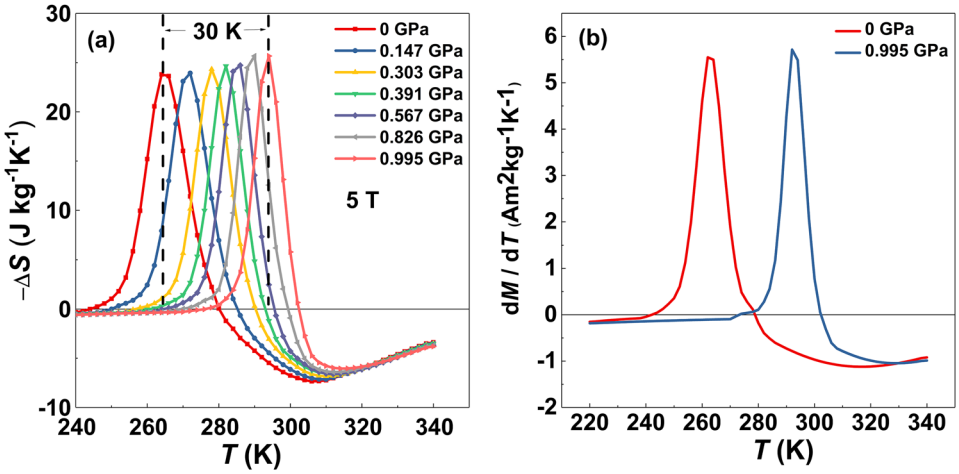

FIG. 2. (a) Entropy change as a function of temperature calculated by Maxwell equation for a magnetic change of 5–0 T at different pressures: 0, 0.147, 0.303, 0.393, 0.567, 0.826, 0.995 GPa (b) dM/dT-T for 0 GPa and 0.995 GPa deduced from Fig. 1(a).

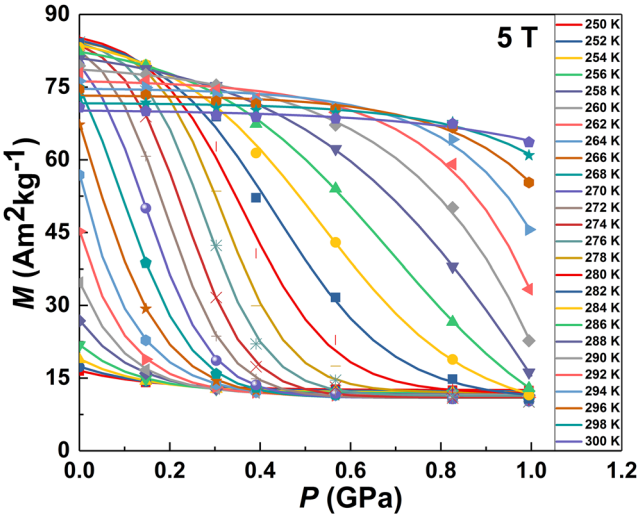

FIG. 3. Magnetization as a function of pressure in the transition temperature region at a magnetic field of 5 T, where dots correspond to experimental data and lines correspond to the fitted data.

assume the relationship between the magnetization and the pressure is as follows in the phase transition region ($Pt - \delta P \le P \le Pt + \delta P$, here Pt denotes the critical pressure inducing phase transition at a certain temperature):

$$M(T, 5\,\mathrm{T}, P) = \frac{1}{2}[M_{FM} + M_{PM}] + \frac{1}{2}[M_{FM} - M_{PM}]\tanh\left(\frac{a - P}{b}\right), \tag{7}$$

where M_{FM} and M_{PM} denote the magnetization of the FM and PM phases, respectively. The parameters a and b are the ones involving the change of phase transition width and shape relative to pressure at the 5 T magnetic field.

Beyond the phase transition region, an exponential function is used to describe the relationship between the magnetization and the pressure at a specific temperature as follows:[9]

$$M(T, 5\,\mathrm{T}, P) = M_{PM} + [M(T, 5\,\mathrm{T}, P - \delta P) - M_{PM}]\exp\left(\frac{P - a_1}{b_1}\right), \quad P < Pt - \delta P, \tag{8}$$

$$M(T, 5\,\mathrm{T}, P) = M_{FM} + [M(T, 5\,\mathrm{T}, P + \delta P) - M_{FM}]\exp\left(\frac{a_2 - P}{b_2}\right), \quad P > Pt + \delta P. \tag{9}$$

Figure 3 shows the magnetization as a function of pressure (M-P curves) in the phase transition temperature region (250–300 K) at the 5 T magnetic field, where dots represent the measured data, and the lines represent the data obtained from the nonlinear fitting. As shown, the fitted data is basically consistent with the measured data.

According to the fitted results shown in Fig. 3, we calculated the relationship of the magnetic volume coupling coefficient $\chi_{12} = \left(\frac{\partial M}{\partial P}\right)_{T,\mu_0 H}$ with P and T under the constant magnetic field of 5 T. The results are shown in Figs. 4(a) and 4(b) in a colored contour map and two-dimensional plots, respectively. At a constant temperature during the phase transition region, the specimen transfers from the ferromagnetic austenite phase to the paramagnetic martensitic phase in the process of increasing pressure. Hence, magnetization decreases, indicating the magnetic volume coupling coefficient χ_{12} is negative. From Figs. 4(a) and 4(b), one can note that the χ_{12} peaks at 264 K under 0 GPa, exactly the same as the martensitic temperature T_M under 0 GPa. As the pressure increases, the peak position of χ_{12} gradually moves to high temperatures, while the peak value of $|\chi_{12}|$ decreases first and then increases. When the pressure reaches 0.995 GPa, the peak position of χ_{12} also locates exactly at the $T_M \sim 294$ K. This result indicates that the magnetic volume coupling coefficient χ_{12} always exhibits peaks around T_M regardless of the pressure. In other words, the most temperature-sensitive position during phase transition also behaves the most pressure-sensitive, reflecting the characteristics of magnetic volume coupling during

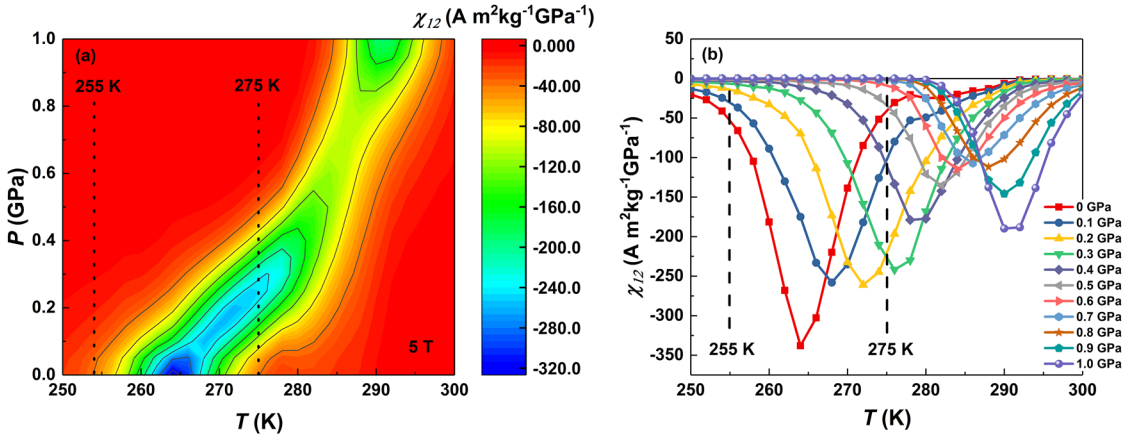

FIG. 4. (a) Colored contour map and (b) two-dimensional plots of magnetic volume coupling coefficient ($\chi_{12} = \left(\frac{\partial M}{\partial P}\right)_{T,\mu_0 H}$) as functions of pressure and temperature.

phase transition. In addition, as shown in Fig. 4, under the pressure of 0 GPa, χ_{12} behaves negative only between 255 K and 275 K because the phase transition completes in this temperature region. When the hydrostatic pressure reaches and exceeds 0.4 GPa, χ_{12} approaches 0 throughout this region from 255 K to 275 K because the phase transition region moves higher and almost no overlap occurs with that under 0 GPa. From Eq. (5), we know that the coupled caloric effect (ΔS_{cp}) is the double integral of χ_{12} against the magnetic field and the pressure. Accordingly, the specific behavior of χ_{12} as functions of P and T will have a direct influence on the expression of coupled caloric effect.

Figure 5(a) shows the three-dimensional diagram of the coupled caloric effect $(\Delta S_{cp}(T, P, 5\,\mathrm{T} \rightarrow 0) = \int_0^P \int_{\mu_0 H_1}^{\mu_0 H_2} \frac{\partial \chi_{12}}{\partial T} dP' d(\mu_0 H'))$ as functions of P and T under a magnetic field change of 5–0 T calculated by Eq. (5). For clarity, we also present a two-dimensional plot in Fig. 5(b), which shows the relationship between the coupled caloric effect and temperature at different pressures. As clearly shown in Fig. 5(a), a negative peak with slowly increasing width and depth gradually develops around 264 K as the pressure increases; meanwhile a positive peak forms in the high temperature region. The negative peak increases but shows saturation as the pressure reaches up to 0.4 GPa, while the positive peak continuously increases and shifts to higher temperatures, and no saturation trend appears even under a pressure of 1 GPa. All these behaviors correspond to the evolution of the magnetic volume coupling coefficient χ_{12} with P and T, as shown in Fig. 4. At 0 GPa, the χ_{12} shows the maximum around $T_M \sim 264$ K, and the coupled caloric effect $\Delta S_{cp}(T, P, 5\,\mathrm{T} \rightarrow 0)$ is zero because no pressure is applied. Owing to the shift of T_M to higher temperature driven by pressure, the χ_{12} around the $T_M \sim 264$ K becomes smaller. Then the double integral of χ_{12}, i.e., $\int_0^P \int_{\mu_0 H_1}^{\mu_0 H_2} \frac{\partial \chi_{12}}{\partial T} dP' d(\mu_0 H')$, results in the appearance and growth of a negative peak of $\Delta S_{cp}(T, P, 5\,\mathrm{T} \rightarrow 0)$ around the $T_M \sim 264$ K, which compensates the entropy change under 0 pressure and makes the entropy change to be 0 around the $T_M \sim 264$ K when the pressure reaches $P = 0.4$ GPa (Fig. 6). This negative peak of $\Delta S_{cp}(T, P, 5\,\mathrm{T} \rightarrow 0)$ remains nearly unchanged when the pressure $P > 0.4$ GPa, noting that the entropy change already becomes 0 around the $T_M \sim 264$ K and no more compensation is required. By contrast, the positive peak of $\Delta S_{cp}(T, P, 5\,\mathrm{T} \rightarrow 0)$ keeps rising and moving to higher temperature with increasing pressure. This is the result dominated by the behavior of the magnetic volume coupling coefficient χ_{12}, as shown in Fig. 4. The continuous increase of the $\Delta S_{cp}(T, P, 5\,\mathrm{T} \rightarrow 0)$ peak reflects the evolution of magnetic-structural coupling with pressure, which contributes to the enhanced entropy change at high pressure. One can note that the peak value of this ΔS_{cp} can be as high as 25.7 J kg^{-1} K^{-1} around the $T_M \sim 294$ K when the applied pressure is up to 1 GPa.

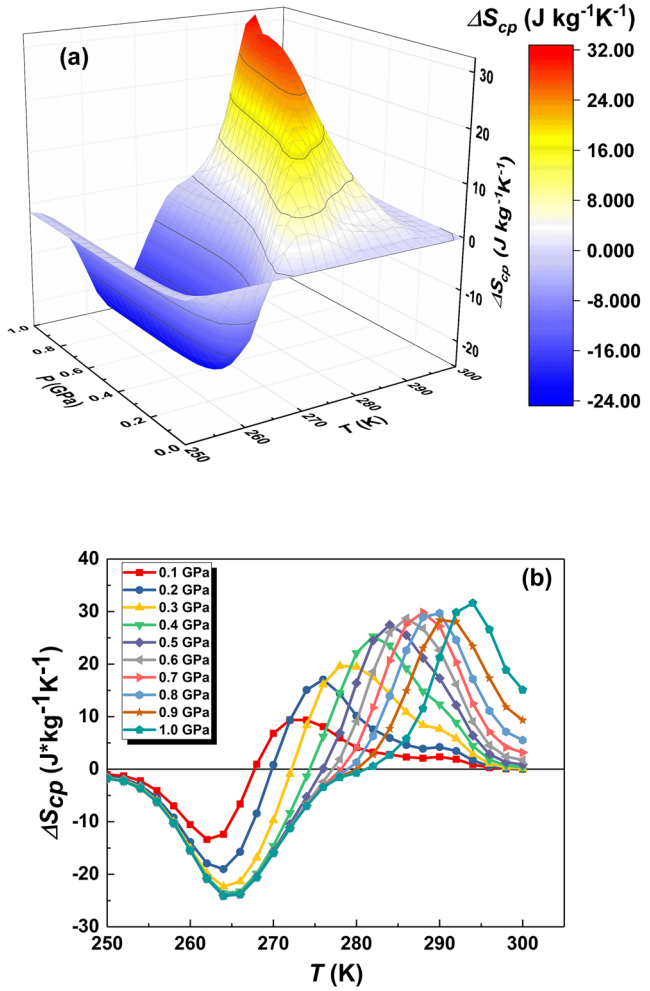

FIG. 5. (a) Three-dimensional and (b) two-dimensional plots of the coupled caloric effect $(\Delta S_{cp}(T, P, 5\,\mathrm{T} \rightarrow 0) = \int_0^P \int_{\mu_0 H_1}^{\mu_0 H_2} \frac{\partial \chi_{12}}{\partial T} dP' d(\mu_0 H'))$ as a function of pressure and temperature under a magnetic field change of 5–0 T.

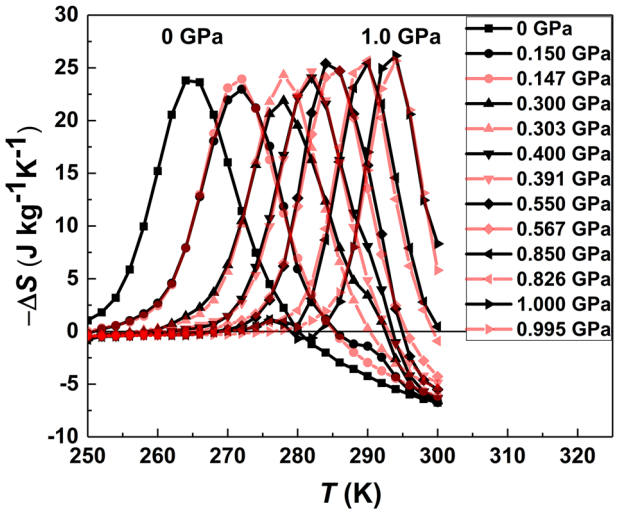

FIG. 6. Comparison of the entropy change at ambient pressure adjusted by the coupled effect [$\Delta S_{0\mathrm{GPa}}(T, 5\,\mathrm{T} \rightarrow 0) + \Delta S_{cp}(T, P, 5\,\mathrm{T} \rightarrow 0)$, black curves] and magnetocaloric results at a specific pressure [$\Delta S(T, P, 5\,\mathrm{T} \rightarrow 0)$, red curves] calculated using Maxwell's relation.

To confirm the rationality of the calculated coupled caloric effect, we compared the results of the entropy change at ambient pressure adjusted by the coupled caloric effect [$\Delta S_{0\mathrm{GPa}}(T, 5\ \mathrm{T} \rightarrow 0) + \Delta S_{cp}(T, P, 5\ \mathrm{T} \rightarrow 0)$] and the magnetocaloric effects calculated using Maxwell's relation under different pressures, as shown in Fig. 6. It can be seen that the entropy change at ambient pressure adjusted by the coupled caloric effect [$\Delta S_{0\mathrm{GPa}}(T, 5\ \mathrm{T} \rightarrow 0) + \Delta S_{cp}(T, P, 5\ \mathrm{T} \rightarrow 0)$, black curve] and magnetocaloric results under specific pressures [$\Delta S(T, P, 5\ \mathrm{T} \rightarrow 0)$, red curve] are basically the same, which is consistent with the description in Eq. (5). That is to say, the thermal effect driven by magnetic field under a certain pressure is the magnetocaloric effect at ambient pressure adjusted by the coupled caloric effect; thus, the nature of the pressure regulated phase transition temperature region and the enhanced entropy change has been explained.

In summary, we investigated the multicaloric and coupled caloric effect driven by magnetic field and pressure in the metamagnetic shape memory alloy $Ni_{50}Mn_{35}In_{15}$ by means of magnetic measurements under pressure. Studies show that the application of pressure favors the antiferromagnetic coupling in the Mn-rich specimen, behaving in a pressure-driven magnetostructural transition in the phase transition temperature region. Theoretical analysis indicates that the expression of the coupled caloric effect is totally determined by the magnetic volume coupling coefficient χ_{12}. Experiments reveal that the most temperature-sensitive position during phase transition also behaves as the most pressure-sensitive; hence, the χ_{12} always keeps the largest around the T_M and its peak shifts to high temperature with increasing pressure. The specific characteristic of χ_{12} directs the behavior of coupled caloric effect ΔS_{cp}. In particular, the positive peak of ΔS_{cp} keeps rising and moving to higher temperature with increasing pressure, resulted from the strengthened magnetic volume coupling with pressure. The contribution of ΔS_{cp} makes the entropy change increase by 8% though the magnetization change (ΔM) across martensitic transition reduces by 20% when a pressure of 0.995 GPa is applied. Via quantitatively analyzing the χ_{12}, the essence of regulated magnetocaloric effect by pressure is revealed, which is of significance for designing new materials based on the magnetostructural coupling strength and its sensitivity to pressure.

This work was supported by the National Key R&D Program of China (Grant Nos. 2017YFB0702702, 2018YFA0305704, 2017YFA0303601, 2017YFA0206300, and 2016YFB0700903), the National Natural Sciences Foundation of China (Grant Nos. 51531008, U1832219, 51771223, 51590880, and 11674378), Fujian Institute of Innovation (Grant Nos. FJCXY18040303 and FJCXY18040302), and the Strategic Priority Research Program (B) and Key Program of Chinese Academy of Sciences.

REFERENCES

[1] V. K. Pecharsky and K. A. Gschneidner, Jr., "Giant magnetocaloric effect in $Gd_5(Si_2Ge_2)$," Phys. Rev. Lett. **78**, 4494–4497 (1997).
[2] F.-x. Hu, B.-g. Shen, J.-r. Sun, Z.-h. Cheng, G.-h. Rao, and X.-x. Zhang, "Influence of negative lattice expansion and metamagnetic transition on magnetic entropy change in the compound $LaFe_{11.4}Si_{1.6}$," Appl. Phys. Lett. **78**, 3675–3677 (2001).
[3] H. Wada and Y. Tanabe, "Giant magnetocaloric effect of $MnAs_{1-x}Sb_x$," Appl. Phys. Lett. **79**, 3302–3304 (2001).
[4] F.-x. Hu, B.-g. Shen, J.-r. Sun, and G.-h. Wu, "Large magnetic entropy change in a Heusler alloy$Ni_{52.6}Mn_{23.1}Ga_{24.3}$ single crystal," Phys. Rev. B **64**, 132412 (2001).
[5] L. Manosa, D. Gonzalez-Alonso, A. Planes, M. Barrio, J. L. Tamarit, I. S. Titov, M. Acet, A. Bhattacharyya, and S. Majumdar, "Inverse barocaloric effect in the giant magnetocaloric La-Fe-Si-Co compound," Nat. Commun. **2**, 595 (2011).
[6] L. Manosa, D. Gonzalez-Alonso, A. Planes, E. Bonnot, M. Barrio, J. L. Tamarit, S. Aksoy, and M. Acet, "Giant solid-state barocaloric effect in the Ni–Mn–In magnetic shape-memory alloy," Nat. Mater. **9**, 478–481 (2010).
[7] Y. H. Qu, D. Y. Cong, S. H. Li, W. Y. Gui, Z. H. Nie, M. H. Zhang, Y. Ren, and Y. D. Wang, "Simultaneously achieved large reversible elastocaloric and magnetocaloric effects and their coupling in a magnetic shape memory alloy," Acta Mater. **151**, 41–55 (2018).
[8] L. Mañosa, X. Moya, A. Planes, O. Gutfleisch, J. Lyubina, M. Barrio, J.-L. Tamarit, S. Aksoy, T. Krenke, and M. Acet, "Effects of hydrostatic pressure on the magnetism and martensitic transition of Ni–Mn–In magnetic superelastic alloys," Appl. Phys. Lett. **92**, 012515 (2008).
[9] E. Stern-Taulats, T. Castán, A. Planes, L. H. Lewis, R. Barua, S. Pramanick, S. Majumdar, and L. Mañosa, "Giant multicaloric response of bulk $Fe_{49}Rh_{51}$," Phys. Rev. B **95**, 104424 (2017).
[10] H. Meng, B. Li, W. Ren, and Z. Zhang, "Coupled caloric effects in multiferroics," Phys. Lett. A **377**, 567–571 (2013).
[11] A. Planes, T. Castán, and A. Saxena, "Thermodynamics of multicaloric effects in multiferroics," Philos. Mag. **94**, 1893–1908 (2014).
[12] E. Stern-Taulats, T. Castán, L. Mañosa, A. Planes, N. D. Mathur, and X. Moya, "Multicaloric materials and effects," MRS Bull. **43**, 295–299 (2018).
[13] J. Liu, T. Gottschall, K. P. Skokov, J. D. Moore, and O. Gutfleisch, "Giant magnetocaloric effect driven by structural transitions," Nat. Mater. **11**, 620–626 (2012).
[14] J. Kübler, A. R. William, and C. B. Sommers, "Formation and coupling of magnetic moments in Heusler alloys," Phys. Rev. B **28**, 1745–1755 (1983).
[15] E. Şaşıoğlu, L. M. Sandratskii, and P. Bruno, "First-principles calculation of the intersublattice exchange interactions and Curie temperatures of the full Heusler alloys Ni_2MnX(X=Ga, In, Sn, Sb)," Phys. Rev. B **70**, 024427 (2004).
[16] E. Şaşıoğlu, L. M. Sandratskii, and P. Bruno, "Role of conduction electrons in mediating exchange interactions in Mn-based Heusler alloys," Phys. Rev. B **77**, 064417 (2008).
[17] Y. Sutou, Y. Imano, N. Koeda, T. Omori, R. Kainuma, K. Ishida, and K. Oikawa, "Magnetic and martensitic transformations of NiMnX(X=In, Sn, Sb) ferromagnetic shape memory alloys," Appl. Phys. Lett. **85**, 4358 (2004).
[18] A. Planes, L. Manosa, and M. Acet, "Magnetocaloric effect and its relation to shape-memory properties in ferromagnetic Heusler alloys," J. Phys.: Condens. Matter **21**, 233201 (2009).
[19] I. Dubenko, N. Ali, S. Stadler, A. Zhukov, V. Zhukova, B. Hernando, V. Prida, V. Prudnikov, E. Gan'shina, and A. Granovsky, "Magnetic, magnetocaloric, magnetotransport, and magneto-optical properties of Ni–Mn–In-Based Heusler alloys: Bulk, ribbons, and microwires," in *Novel Functional Magnetic Materials: Fundamentals and Applications*, Series in Materials Science (Springer, 2016), Chap. II, Vol. 231, pp. 41–83.
[20] A. K. Pathak, I. Dubenko, S. Stadler, and N. Ali, "The effect of partial substitution of in by Si on the phase transitions and respective magnetic entropy changes of $Ni_{50}Mn_{35}In_{15}$ Heusler alloy," J. Phys. D: Appl. Phys. **41**, 202004 (2008).
[21] S. Zuo, F. Liang, Y. Zhang, L. Peng, J. Xiong, Y. Liu, L. Rui, T. Zhao, J. Sun, F. Hu, and B. Shen, "Zero-field skyrmions generated via premartensitic transition in $Ni_{50}Mn_{35.2}In_{14.8}$ alloy," Phys. Rev. Mater. **2**, 104408 (2018).
[22] W. Eerenstein, N. D. Mathur, and J. F. Scott, "Multiferroic and magnetoelectric materials," Nature **442**, 759–765 (2006).
[23] L. Tocado, E. Palacios, and R. Burriel, "Entropy determinations and magnetocaloric parameters in systems with first-order transitions: Study of MnAs," J. Appl. Phys. **105**, 093918 (2009).
[24] B. Kaeswurm, V. Franco, K. P. Skokov, and O. Gutfleisch, "Assessment of the magnetocaloric effect in La, Pr(Fe, Si) under cycling," J. Magn. Magn. Mater. **406**, 259–265 (2016).
[25] A. Magnus, G. Carvalho, A. A. Coelho, P. J. von Ranke, and C. S. Alves, "The isothermal variation of the entropy (ΔST) may be miscalculated from magnetization isotherms in some cases: MnAs and $Gd_5Ge_2Si_2$ compounds as examples," J. Alloys Compd. **509**, 3452–3456 (2011).

[26]S. Aksoy, M. Acet, P. P. Deen, L. Mañosa, and A. Planes, "Magnetic correlations in martensitic Ni–Mn-based Heusler shape-memory alloys: Neutron polarization analysis," Phys. Rev. B **79**, 212401 (2009).
[27]V. V. Khovaylo, T. Kanomata, T. Tanaka, M. Nakashima, Y. Amako, R. Kainuma, R. Y. Umetsu, H. Morito, and H. Miki, "Magnetic properties of $Ni_{50}Mn_{34.8}In_{15.2}$ probed by Mössbauer spectroscopy," Phys. Rev. B **80**, 144409 (2009).
[28]Y. H. Qu, D. Y. Cong, X. M. Sun, Z. H. Nie, W. Y. Gui, R. G. Li, Y. Ren, and Y. D. Wang, "Giant and reversible room-temperature magnetocaloric effect in Ti-doped Ni–Co–Mn–Sn magnetic shape memory alloys," Acta Mater. **134**, 236–248 (2017).
[29]T. Gottschall, D. Benke, M. Fries, A. Taubel, I. A. Radulov, K. P. Skokov, and O. Gutfleisch, "A matter of size and stress: Understanding the first-order transition in materials for solid-state refrigeration," Adv. Funct. Mater. **27**, 1606735 (2017).